

A machine learning-based integration of flow cytometry, 16S rRNA gene sequencing, and productivity data to associate bacterial taxa with functional groups: Supporting Information

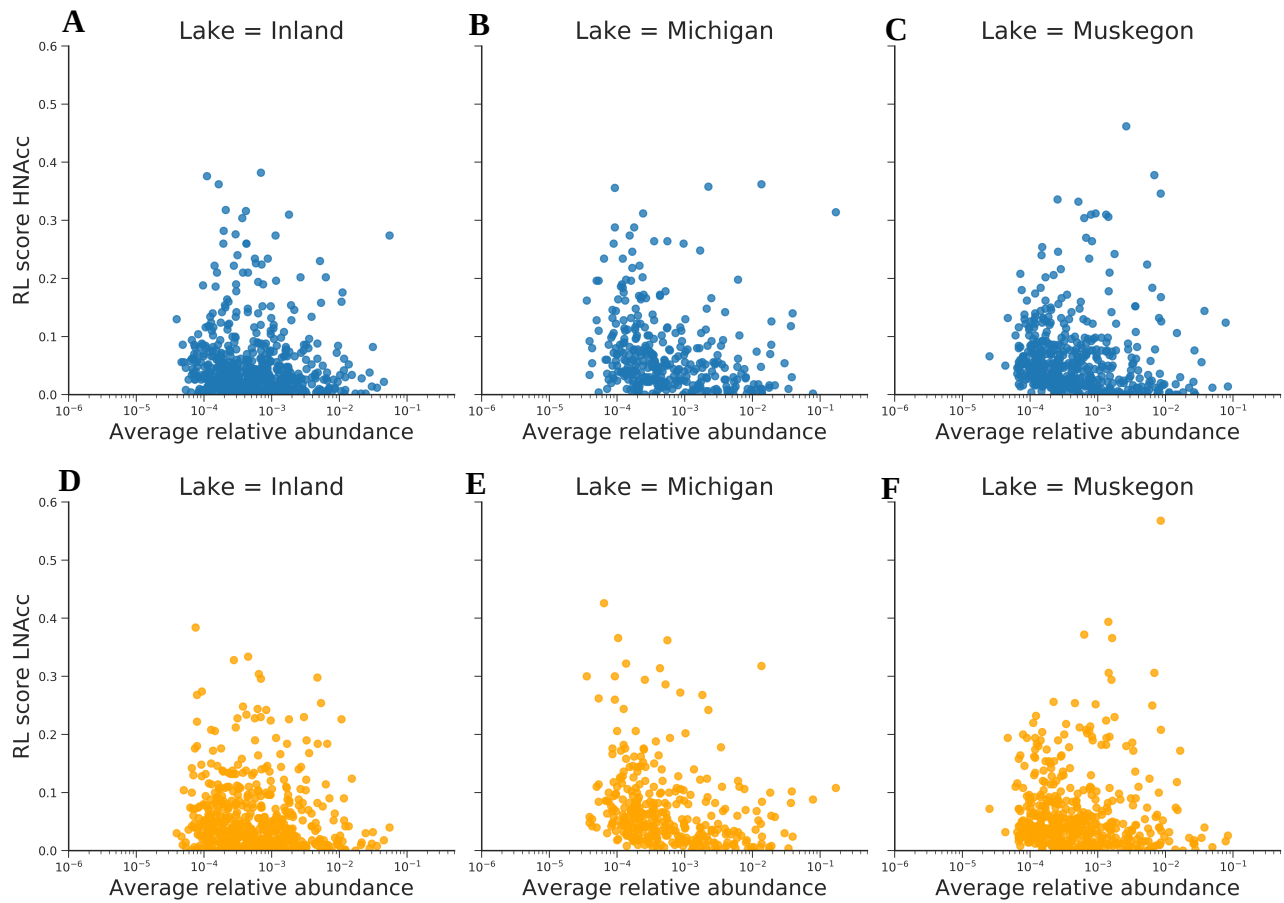


Figure S1: Scatter plot of RL score versus the average relative abundance of every OTU for HNAcc (blue points, **A**, **B** and **C**) and LNAcc (orange points, **D**, **E** and **F**) for each lake system: Inland (**A** and **D**), Michigan (**B** and **E**) and Muskegon (**C** and **F**).

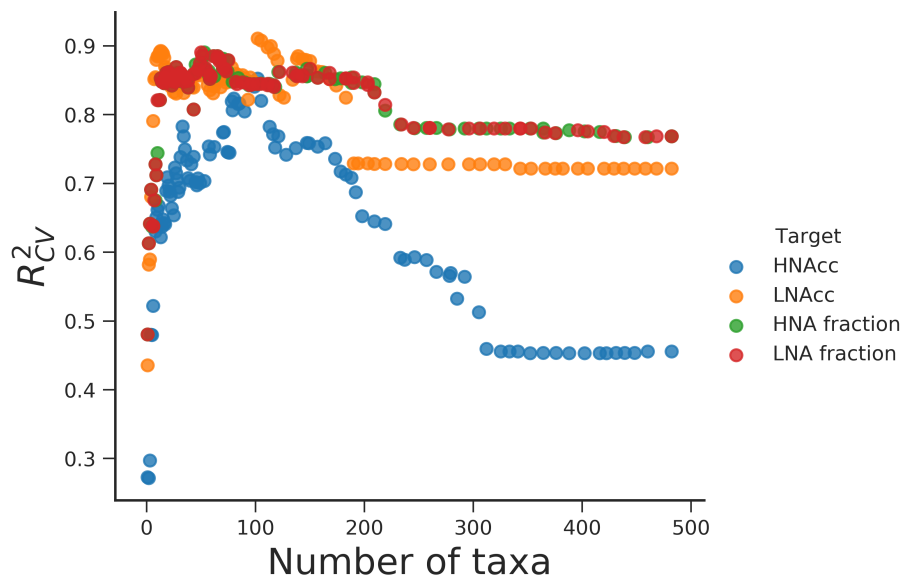


Figure S2: Comparison of predictions of HNAcc and LNAcc versus relative fractions. This was done for lake Muskegon at the OTU level, expressed in terms of R^2_{CV} . The subset of taxonomic variables was iteratively reduced using a recursive variable elimination strategy, based on the RL score. Lowest-scored variables were removed at every step, after which the base model (i.e., the Lasso) was used to model and predict cell counts or fractions. Predictions for HNA and LNA fractions overlap (red and green dots).

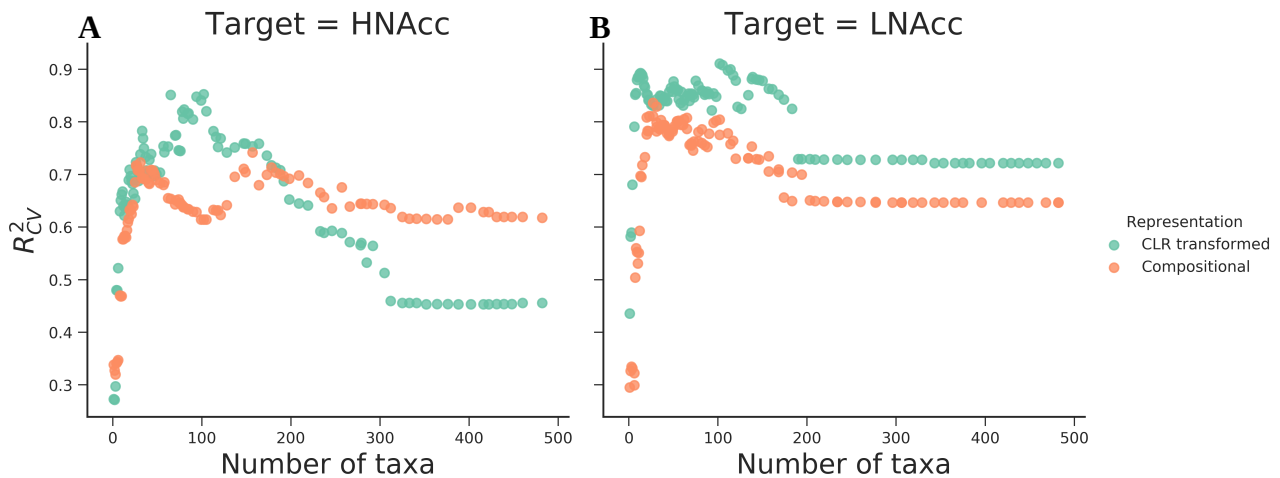


Figure S3: Prediction of HNAcc (A) and LNAcc (B) for lake Muskegon at the OTU level, expressed in terms of R^2_{CV} using relative abundances ('compositional') and CLR transformed ('CLR transformed'). The subset of taxonomic variables was iteratively reduced using a recursive variable elimination strategy, based on the RL score. Lowest-scored variables were removed at every step, after which the base model (i.e., the Lasso) were used to model and predict HNAcc and LNAcc.

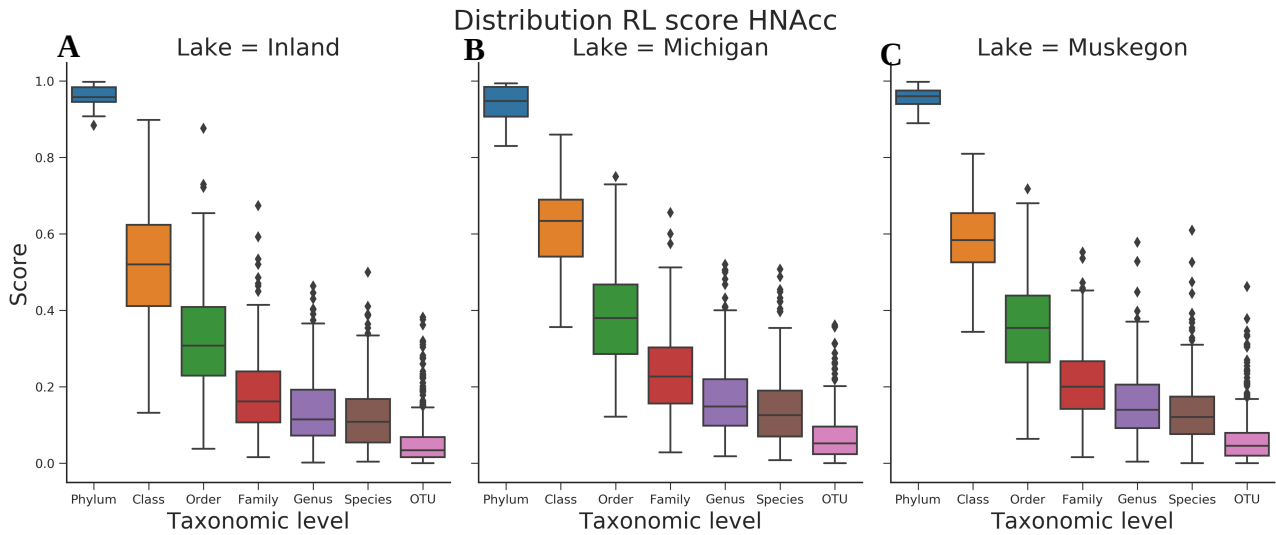


Figure S4: Distribution of the RL score for all lake systems (**A**: Inland, **B**: Michigan and **C**: Muskegon) and all taxonomic levels in function of HNAcc.

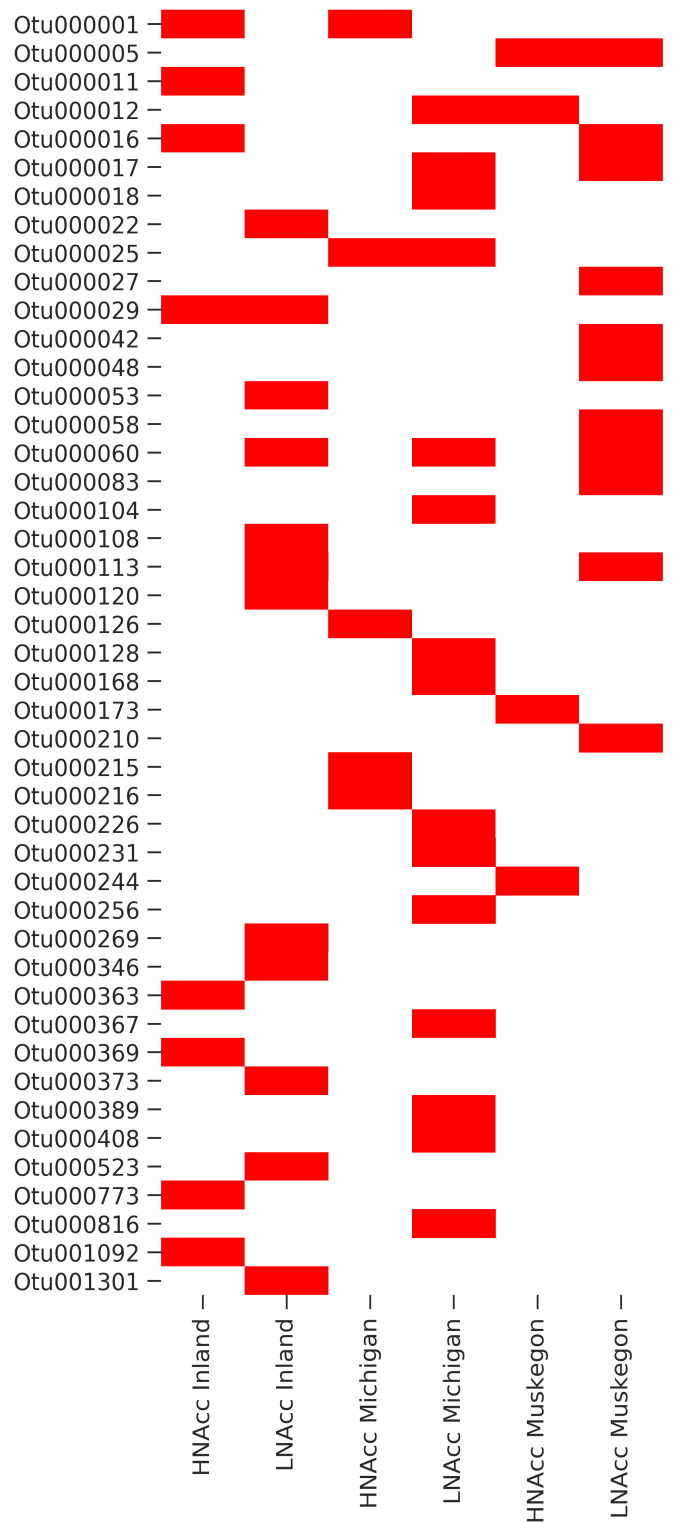


Figure S5: Selected OTU's (in red) according to the Boruta algorithm for each lake system and functional group.

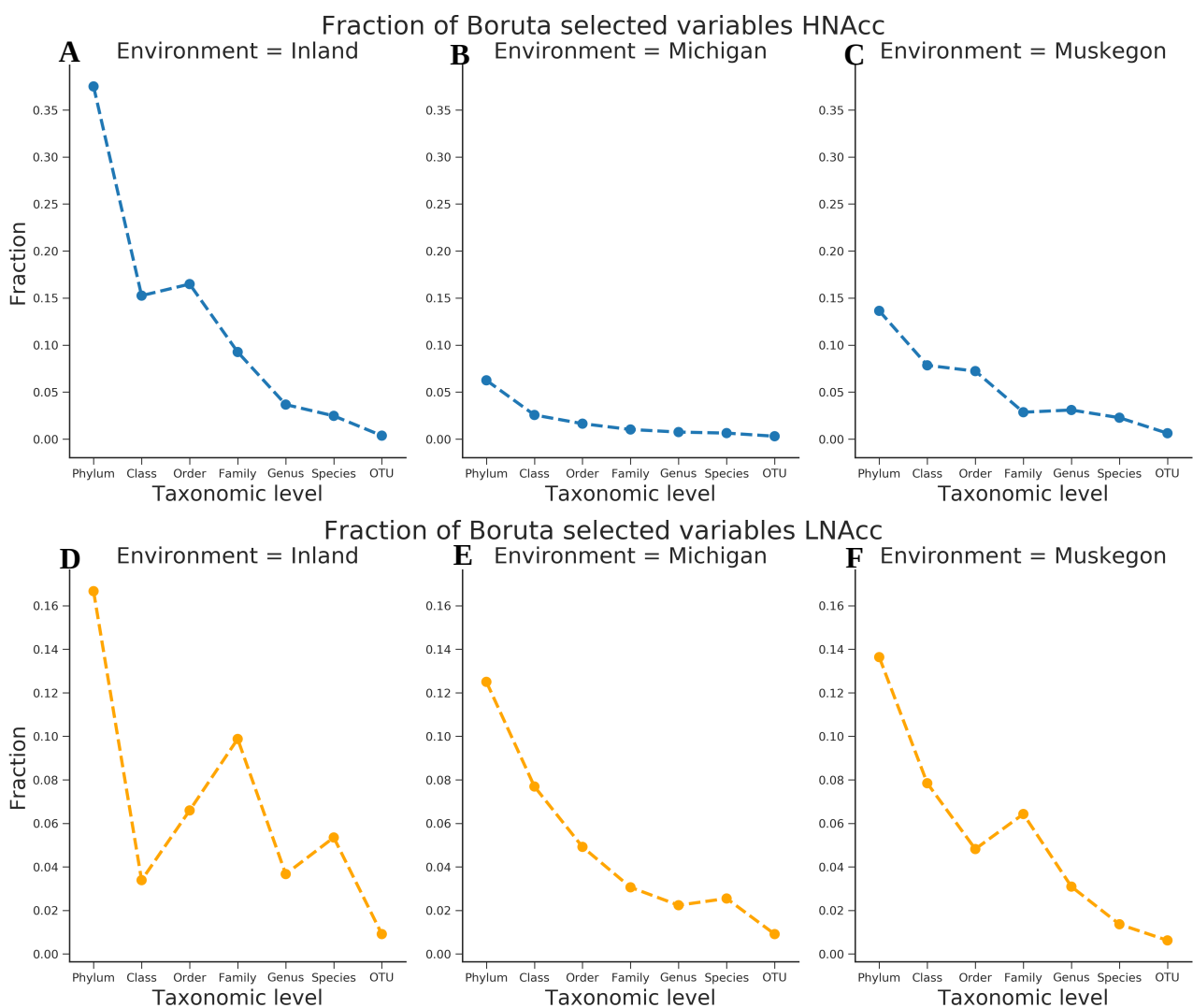


Figure S6: Relative fraction of selected OTUs using the Boruta algorithm for HNAcc (blue points, **A, B** and **C**) and LNAcc (orange points, **D, E** and **F**) for each lake system: Inland (**A** and **D**), Michigan (**B** and **E**) and Muskegon (**C** and **F**).

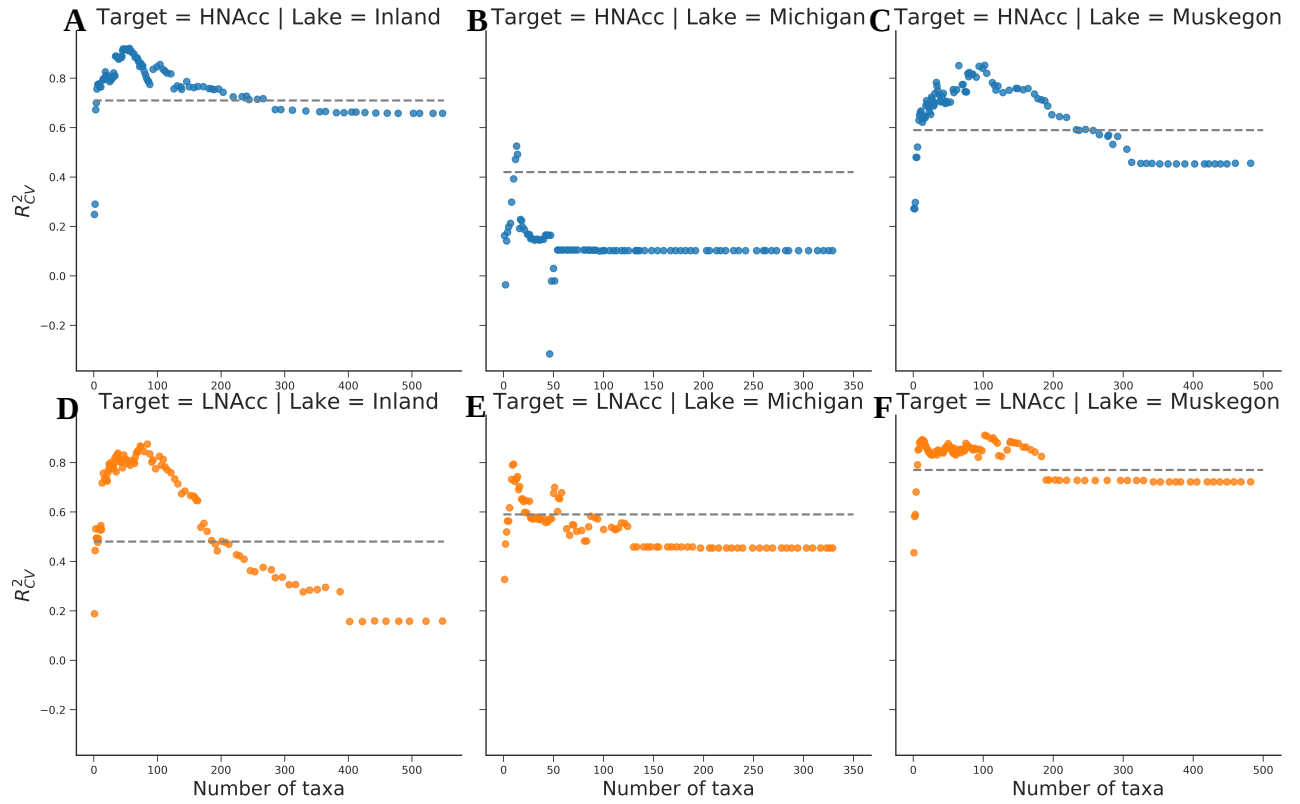


Figure S7: Comparison of Random Forest predictions (grey dashed line) using Boruta selected OTU's versus predictions using the Lasso and RL score for HNAcc (blue points, **A**, **B** and **C**) and LNAcc (orange points, **D**, **E** and **F**) for each lake system: Inland (**A** and **D**), Michigan (**B** and **E**) and Muskegon (**C** and **F**). Performance is expressed in terms of R^2_{CV} .

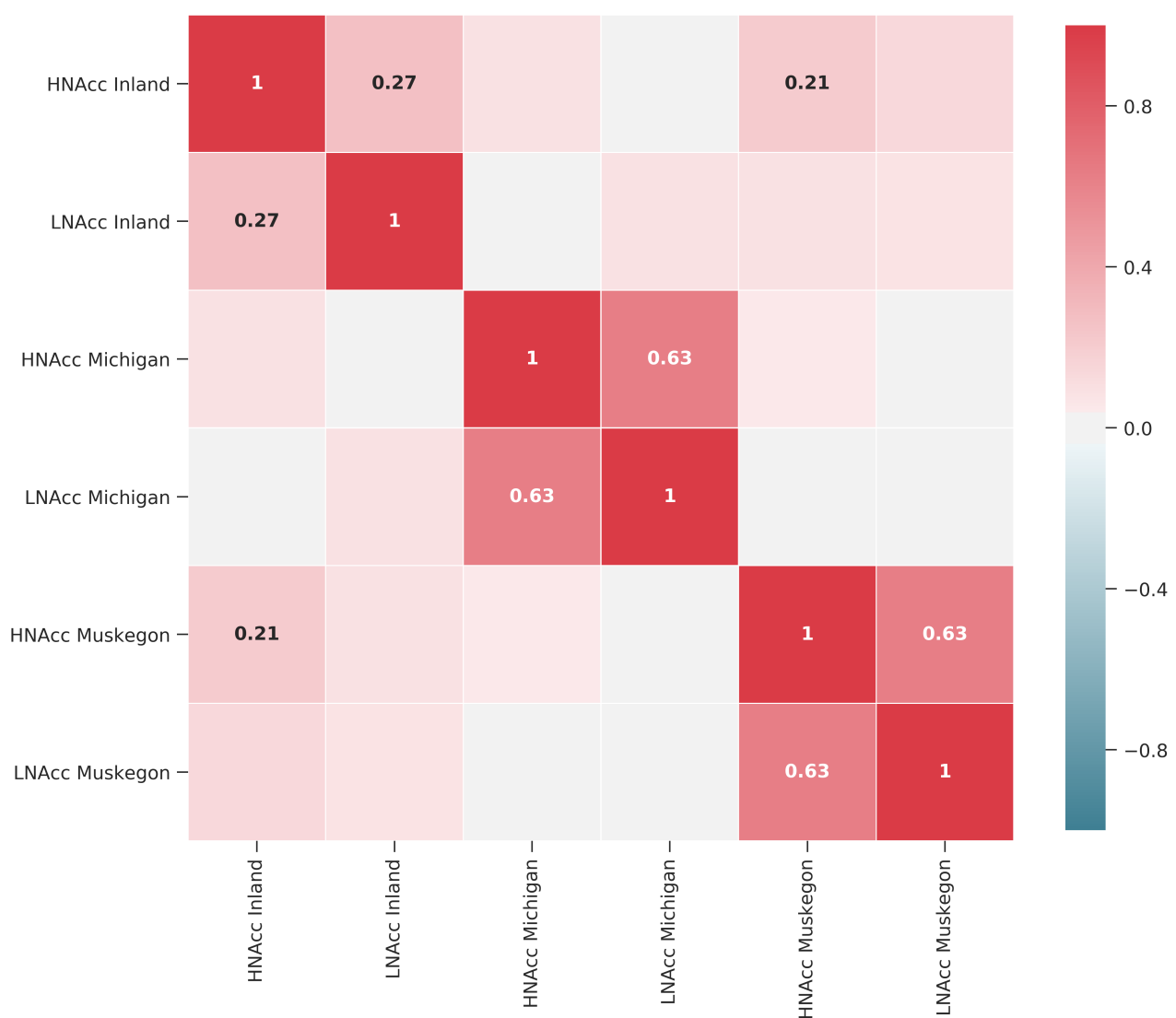


Figure S8: Pearson correlations between RL scores assigned to OTUs in function of HNAcc and LNAcc between lake systems. Only those OTUs were considered that were present in all lake systems, which were 190 in total. Values are bolded if $P < 0.05$.

Tree scale: 0.1

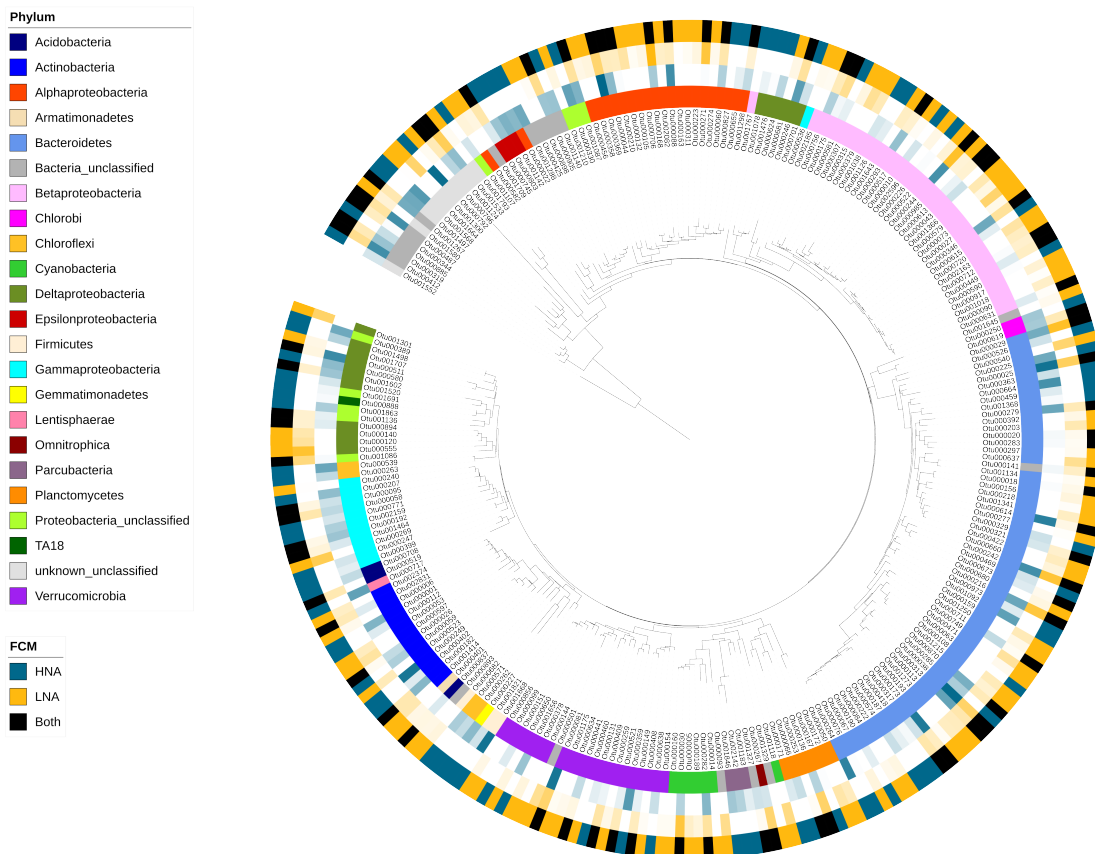


Figure S9: Phylogenetic tree with all HNA and LNA selected OTUs from each of the three lake systems with their phylum level taxonomic classification (first row) and association with HNA, LNA or to both groups based on the RL score threshold values (last row). Second (HNA) and third row (LNA) display RL scores.

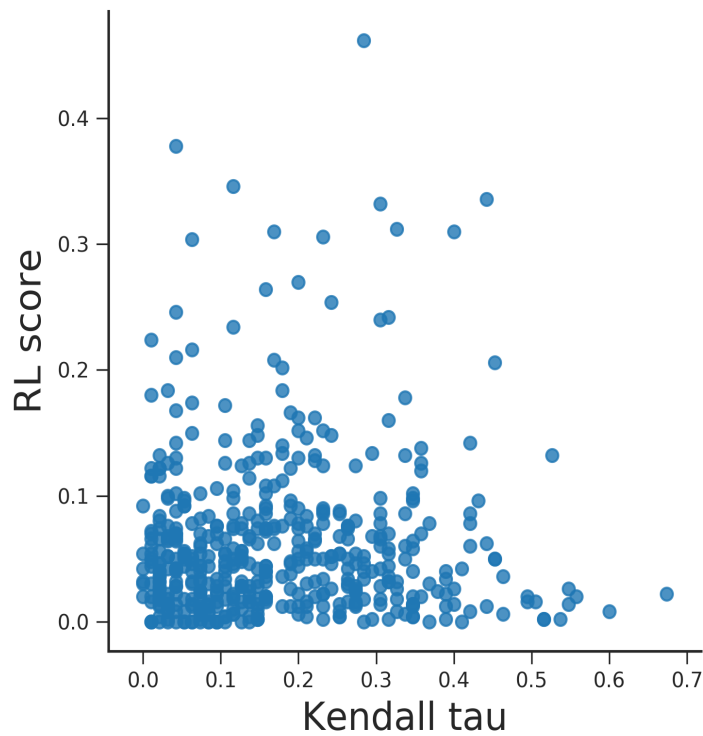


Figure S10: Kendall's tau of individual OTU abundances and productivity measurements versus the RL score, determined in function of HNAcc.

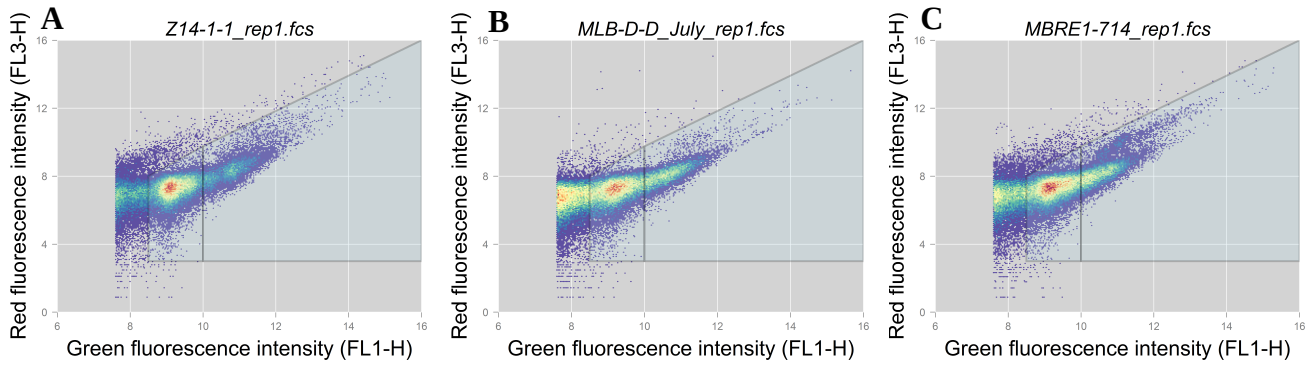


Figure S11: Examples of the gating strategy to determine HNAcc and LNAcc for the three lake systems. The gating strategy is performed in the $\text{arcsinh}(x)$ transformed bivariate space of the FL1-H and FL3-H channel, following guidelines of Prest et al., 2013. **A:** Inland, **B:** Michigan, **C:** Muskegon.